Using Nail Board Experiments to Quantify Surface Velocity in the CC Mold

Bret Rietow and Brian G. Thomas

University of Illinois at Urbana-Champaign
1206 West Green Street
Urbana, IL 61801
Tel.: 217-333-6919
Fax: 217-244-6534
E-mail: bgthomas@uiuc.edu

Key words: steel, continuous casting; fluid flow, velocity measurement, computational models, mold slag.

INTRODUCTION

Steel quality is greatly affected by the fluid flow pattern in the mold, which is difficult to measure, owing to the harsh molten steel / slag environment and electrical interference, such as from electromagnetic flow control systems. Inserting nail boards into the continuous casting mold through the top surface is a simple, yet powerful tool to gain this important information. Nailboard measurements are commonly used to measure the thickness of the molten slag layer, and the liquid level profile, as pioneered by Dauby and coworkers at LTV Steel [1].

The test is performed by inserting one or two rows of 5~15 steel nails and aluminum wires into a long board, as shown in Fig. 1. The nails are dipped straight down through the slag layer into the top surface of the mold along the center plane between the wide faces, as shown in Fig. 2. They should remain immersed for 3-4s, in order to solidify a thin skull of metal onto the end of each nail. Excessive immersion time may cause problems such as remelting the skull or solidifying the steel surface in the mold. If electromagnetic braking is applied, testing is easier if the nails are stainless steel, in order to avoid electromagnetic forces acting on the nails. After removal, the shape of the skull of steel that has solidified on the end of each nail, and the aluminum wire lengths are measured.

The local depth of the slag layer is indicated by distance from the steel lump to the end of the aluminum wire, which melts back due to its low melting temperature [1, 2]. Fortunately, the slow rate of aluminum melting in the solid powder prevents the aluminum wire from melting much beyond the molten slag interface, if the immersion time is optimal. The profile of all of the nail skull positions plotted together indicates the shape of the steel meniscus during the time of nailboard immersion. This shape of the liquid level provides an indication of the flow pattern beneath. The profile is higher near the SEN for single-roll flow patterns. The profile is higher near the narrow face for double-roll flow patterns, due to the uplifting effect of flow up the narrow face, as pictured in Fig. 1. The extent of uplifting increases with increasing flow velocity up the narrow faces. Thus, the profile difference provides a qualitative estimate of flow velocity, which can be used to provide feedback for electromagnetic flow control with a double-roll flow pattern.

The direction of flow along the top surface can be found by recognizing that the high end of each angled skull represents the instantaneous direction from which steel flow impinges on the nail [3, 4]. Furthermore, the height difference between the high and low ends of the skull profile indicates the magnitude of the local surface velocity [3, 4]. Flow past a submerged column will run up the upstream side of the column, as pictured in the water model test in Fig. 3. The run-up height, $h_{run\text{-}up}$, increases with increasing liquid velocity. In addition, the surface height of the wake of the flow behind the cylinder decreases with increasing liquid velocity. Because run-up height is difficult to determine after a nail-board test, the knob height difference, Δh, between the maximum run-up height and the minimum wake height on the opposite side, is a more practical indicator of liquid velocity (see Figs. 4 and 5). In addition to the steel velocity, these indicators also depend on the nail diameter, D, and the fluid properties, including density, viscosity, and surface tension.

Nailboard tests to measure the slag layer thickness, the steel interface profiles, the surface flow direction, and the surface flow intensity are often applied to learn about flow in the mold [2, 4-9]. Excessive surface velocities lead to slag entrainment defects, while

insufficient velocities lead to meniscus freezing and other defects [5, 6, 10-12]. Single-roll and unstable flow patterns are inferior to a stable double-roll flow pattern with an optimized, intermediate surface flow velocity [2, 12].

The current work shows how to extend the simple nailboard test to quantify the magnitude of the surface velocity. The flow of molten steel and slag around a steel nail immersed into the top of the mold has been simulated using a 3-D model of multiphase flow with a free surface. The model has been extensively validated with both test problems and plant measurements. The velocity of the steel across the top surface of the mold is presented as a function of the height difference of the solidified lump on the nail, and the nail diameter.

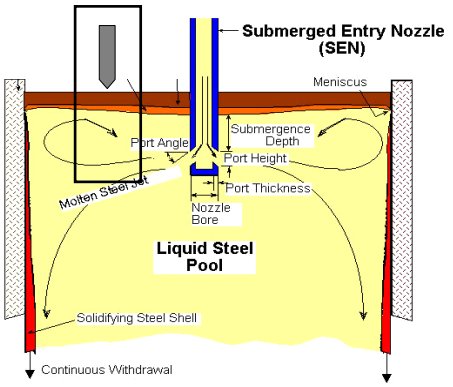

Figure 1. Continuous casting mold showing steel flow, top surface slag layers, and location of nail-board insertion [1)]

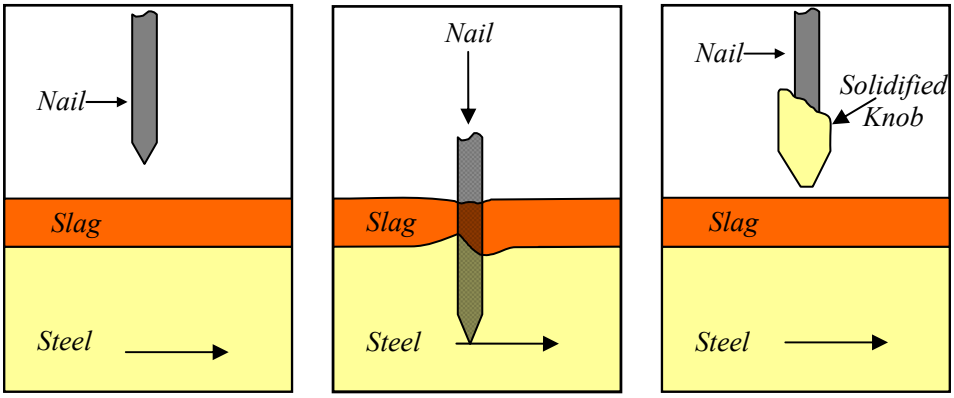

Step 1: Insert nail through Slag layer into liquid pool

Step 2: Hold nail in steel for short time

Step 3: Remove nail, and measure shape of knob

Figure 2. Nailboard method to measure steel surface speed and direction

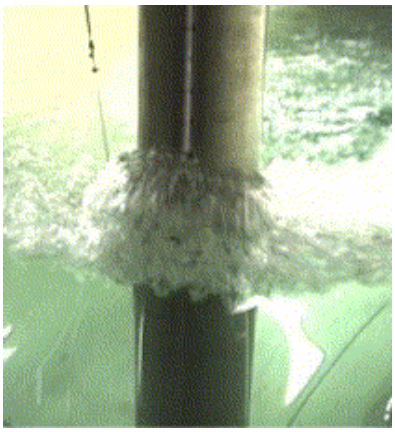

Figure 3. Flow past immersed column in water model

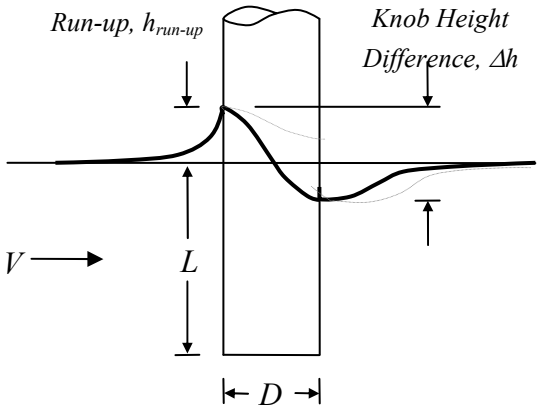

Figure 4. Schematic of flow variables: run-up height and measured knob height difference

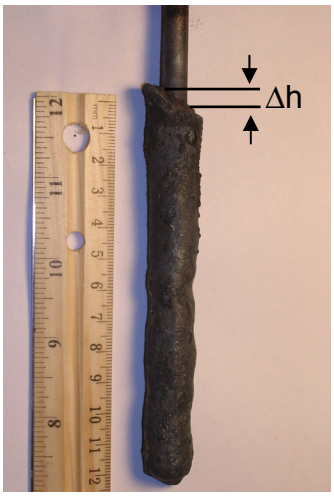

Figure 5. Nail photo showing measurement of solidified knob

METHODS TO MEASURE VELOCITY IN MOLTEN METAL

The hostile environment of molten metal flow beneath a slag layer presents many problems for velocity measurement. Several different methods have been reviewed and evaluated by Argyropoulos and coworkers [13, 14]. Conventional flow meters and immersed probes cannot withstand the high temperatures. Surface visualization methods, such as photographic analysis of moving variations on the exposed surface,[15] are generally prevented by the slow-moving, opaque slag layer that covers the flowing metal. Suspended electromagnetic measurement devices just above the powder layer are promising, but may have difficulties from electronic interference, especially when electromagnetic forces are used to control the flow pattern. Tracer diffusion methods, such as the addition of sulfide, rare earth, or radioactive alloys to the steel[16] requires tedious sampling and composition analysis, and would be

inaccurate for the short time scales involved in mold flow. Argyropoulos [13, 17] developed a method based on immersing steel spheres into the fluid, and measuring the time needed to melt the sphere, which is related to the flow velocity and fluid superheat temperature. This destructive test requires analysis of several sensors embedded in the sphere, so is very labor intensive.

A system of MFC sensors embedded behind the mold walls was developed by AMEPA to measure velocity in continuous slab casters [18]. Speed is computed from the time delay of signals recorded between two fixed probes, due to the propagation of variations in the induced electromagnetic current caused by flow variations in the liquid steel as they through the magnetic fields. This expensive system can only measure average velocity in a region near the solidifying shell, and only in regions, (such as near the top surface), where the flow is uniform and one-dimensional between the two probes [19]. It has been applied successfully to differentiate between flow patterns [2].

A probe based on Von Karman vortex shedding has recently been commercialized to measure horizontal flow velocity at the surface of molten steel [20]. This method immerses a long rod into the top surface and measures the frequency of the vibrations caused by the vortex shedding, which increases directly with flow speed. It requires a rigid support to suspend the sensitive equipment just above the oscillating mold and requires filtering of noise in the signal, which can arise from many sources. A simpler method, that has been used successfully in practice, is to measure the torque or the deflection angle of the rod, which must be refractory-coated to survive in the harsh environment (e.g. Mo-ZrO_2 thermet) [10].

Given these difficulties, extracting quantitative velocity data from simple, inexpensive nail-board tests, is an important innovation.

COMPUTATIONAL MODEL

A three-dimensional model of fluid flow has been developed to simulate the free-surface shape, velocity and pressure fields within a symmetric portion of the top surface of the molten steel, around half of a nail, as shown in Fig. 6. This 3-D domain extends to the nail surface, which comprises part of the edge of the domain near the centerplane. For most simulations, the domain also includes the molten slag layer, which introduces another arbitrarily-shaped interface, which defines the initial profile of the solidified knob where it intersects with the nail boundary. The computational model solves the standard 3-D incompressible Navier-Stokes equations for the conservation of mass and momentum in each phase in an Eulerian reference frame:

$$\frac{\partial}{\partial x_i}\left(\overline{u_i}\right) = 0 \;; \qquad \rho\left(\frac{\partial \overline{u_i}}{\partial t} + \frac{\partial}{\partial x_j}\left(\overline{u_i u_j} + \overline{u_i' u_j'}\right)\right) = -\overline{p_i} + \mu_{eff}\frac{\partial}{\partial x_j}\left(\frac{\partial \overline{u_i}}{\partial x_j}\right) + \rho b \tag{1}$$

The standard K-ε model is used to incorporate the effects of turbulence, which requires the solution of two more partial differential equations for the scalar fields of turbulent kinetic energy, K, and its dissipation rate, ε. Standard wall-law boundary conditions are applied at the nail surface and along the steel / slag interface. Reasonable estimates were made for K and ε at the inlet plane [21]. The powder layer above the liquid slag layer is assumed to exert a uniform pressure.

In addition the effects of gravity (buoyancy), surface tension and pressure forces are included, which requires solving the following additional force balance equations at each point on both the 1) steel / slag interface and 2) top surface slag / powder interface:

$$\sigma_i^1 - \sigma_i^2 = 2\gamma H n_i - \frac{\partial \gamma}{\partial x_i} \tag{2}$$

where σ are stresses (including the normal pressures) which act on each side (1 and 2) of the interface, γ is surface tension, H is mean Gaussian curvature (m^{-1}), n_i is normal to the surface, and x_i are the coordinate directions. The free-surface shape is accounted for by tracking the Volume of Fluid, F, by solving the following equation using the VOF method:

$$\frac{\partial F}{\partial t} + u_{T1}\frac{\partial F}{\partial x_{T1}} + u_{T2}\frac{\partial F}{\partial x_{T2}} = 0 \tag{3}$$

where u and x are velocity and displacement in the tangential directions $T1$ and $T2$. The interface shape is defined using the SPINES method, which solves for the vertical position of the interface nodes, which are allowed to move along pre-defined lines [22].

Although the final solution is the steady-state flow pattern, the equations are very difficult to converge, so a transient solution procedure has been developed using the finite-element method with the fixed surface segregated solver in the commercial package FIDAP [22]. The initial condition is found by solving the steady-state form of this flow problem in a 30-mm deep domain without the slag layer. Next, the elements of the 10-mm thick slag layer are added, and the steel domain is deepened to 60-mm. A simple 2-D

transient simulation is performed with no nail, in order to generate accurate far-field flow parameters to use as the inlet boundary conditions for the case with slag. Finally, a 3-D transient simulation with slag is performed until the solution stops changing, such as shown in Fig. 7. Remeshing is performed at each iteration update, insuring that the new nodal coordinates preserve the aspect ratios between element lengths, in addition to satisfying the interface condition between the steel and slag elements. Inlet flow is parallel to the symmetry plane. Heat transfer and solidification are not modeled, so only the initial shape of the knob profile is computed. This is reasonable because the flow field is established much faster than solidification can occur. The domain size was chosen via many trial and error simulations to ensure that it is large enough that the far-field boundaries have virtually zero velocity gradients. A boundary condition of zero normal flow at the bottom surface is applied to maintain fluid continuity. The nail extends to the bottom of the 70-mm deep domain, so any fluid diverted beneath the nail is assumed to have negligible effect on the free surfaces.

Table I Simulation Properties

Steel Properties		Slag Properties		Domain Size	
Density	7400 kg/m^3	Density	3000 kg/m^3	Length (x)	25 x D
Laminar Viscosity	0.006 kg/m-s	Laminar Viscosity	1.000 kg/m-s	Width (y)	~18.5 x D
Kinematic Viscosity	8.11 x 10^{-7} m^2/s	Kinematic Viscosity	3.33 x 10^{-4} m^2/s	Height (z)	60 mm (steel)
Surface Tension	1.6 J/m^2	Surface Tension	0.65 J/m^2		10 mm (slag)

An optimized mesh of 5760 finite elements was used for the Slag Model. The equations were solved using carefully-chosen relaxation factors of 70-90% of the previous solution, in order to enable convergence. Typical computational times to reach residuals of 10^{-3} with this mesh size for the first steady-state run took approximately 0.2 hours. Computational time for the second transient run was about 12 hours to simulate 10,000 time steps (time step size 0.003s) converging in about 3 iterations per step with final residuals of 10^{-3}. All computations for both models were performed using an IBM POWER4 p690 processor with a computational power of 1.3 GHz. Further details of the solution procedure are provided elsewhere [21].

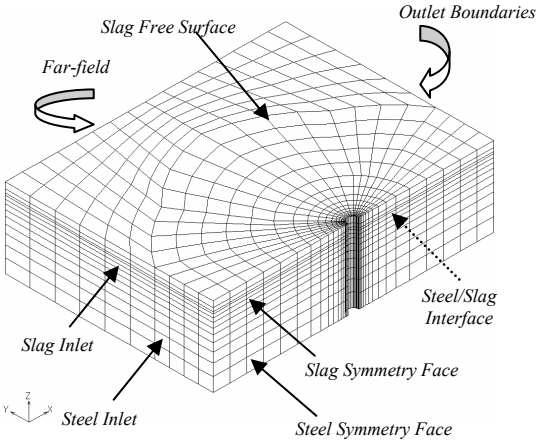

Figure 6. Finite-element Model domain (with slag layer)

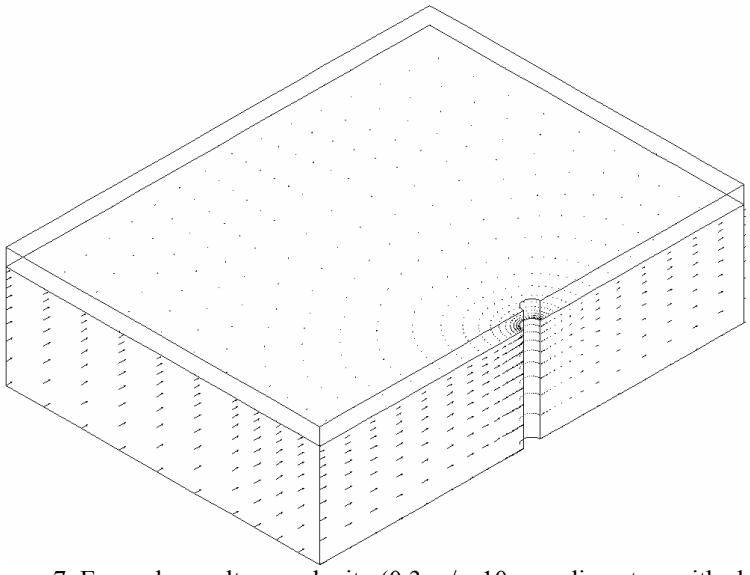

Figure 7. Example results: x-velocity (0.3 m/s; 10-mm diameter; with slag)

MODEL VALIDATION

The ability of the computational model to accurately predict the shape of a moving free surface was first validated with standard test problems, [22] including interface shape in a sloshing tank [23] and flow over a semicircular obstruction[24]. The model was next validated with a test problem of flow past a vertical cylinder of 0.21m diameter in a water model by Chaplin et al [25]. The drag coefficients and run-up height on the leading edge of the cylinder were recorded for different fluid velocities. The run-up height can also be predicted with the Bernoulli equation, which is based on a simple energy balance, converting the kinetic energy of the flowing steel into the potential energy of the run-up height:

$$p + \frac{1}{2}\rho V^2 + \rho g h = C \text{ ; so: } \quad \Delta h_{runup} = \frac{V^2}{2g} \tag{4}$$

The results of all three methods are compared in Figure 8. Two of the cases tested by Chaplin et. al. [25] with similar velocity magnitudes to those experienced at the mold top surface (0.96 and 1.36 m/s) have been used to experimentally validate the model. With a large diameter column, the diameter does not affect the solution, so the theoretical maximum run-up height is achieved.

At very high velocities, flow separation of the run-up and wake regions occurs, as the free surface shape becomes discontinuous, (displayed as the faint dashed profile in Fig. 4). The high-energy fluid produces excessive turbulence, which overcomes the surface tension forces and causes the free surface to break up around the cylinder. This behavior is believed to occur only at surface velocities beyond those encountered in normal continuous casting mold operation, so this effect is neglected in the present work and a continuous free surface profile is assumed.

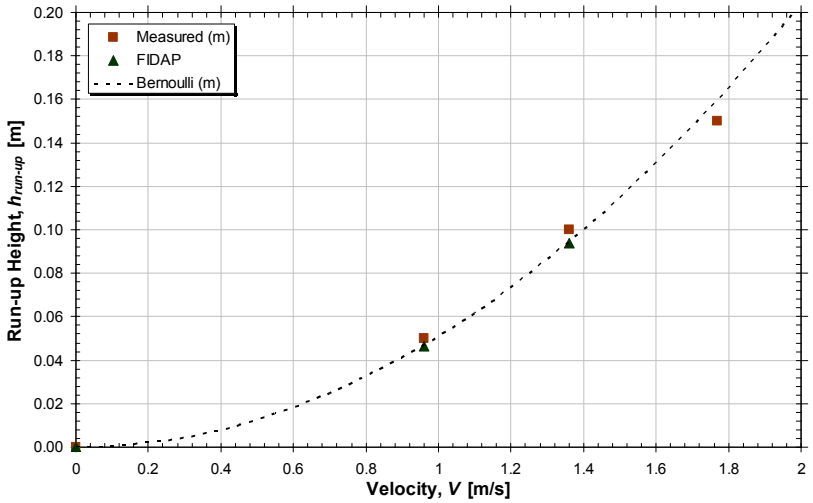

Figure 8. Water-model test problem showing validation of model with measurements and analytical solution

RESULTS

The computational model was applied to simulate over 30 separate cases, which required overcoming many convergence difficulties associated with this complex model. Simulations were performed for 5 different near-surface velocities (0.2 – 0.6 m/s) and 3 different nail diameters, (5, 10, 15mm), both without and with the slag layer on the top surface. Contours of the velocity components, pressure, kinetic energy, dissipation rate, and most importantly, interface shape were plotted for each case. Selected results are shown in Figs. 9 a) and b) for the no-slag and slag cases. Specifically, these figures show how the interface varies around the nail region, lifting up in front, dropping sharply to below the average liquid level, and finally rising gradually back well behind the nail. The far-field edges of the domain are relatively unaffected by the nail, showing that nails can be spaced ~20 nail diameters apart without interfering with each other. The velocity vectors shown in Fig. 7 confirm this. The color contours in these figures show that upward vertical velocity is highest just in front of the nail, due to the run-up flow.

Run-up Height

The simulation results show that run-up height increases consistently with the square of the surface velocity, as plotted in Fig. 10. Increasing nail diameter also increases run-up height. The run-up heights predicted by the computational model approach the upper limit found from the Bernoulli equation, Eq. 4), and have the same trend. At very large diameters, they match exactly, as shown in Fig. 8. Smaller nails enable easier flow around the nail, lessening the conversion of kinetic energy to potential energy, and thereby decreasing the run-up height. At smaller diameters, the effect of nail diameter is almost linear, as Fig. 10 shows that the runup height roughly equals the nail diameter at 0.6m/s. The results without the slag layer are almost identical. Thus, runup height would be the best indicator of surface velocity if the far-field liquid level could be accurately determined.

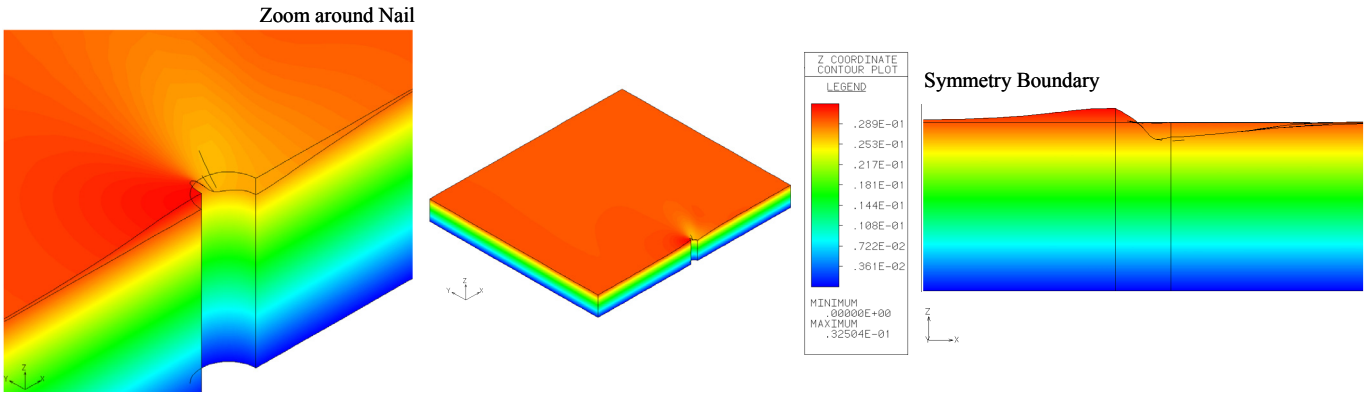

a) Without slag layer

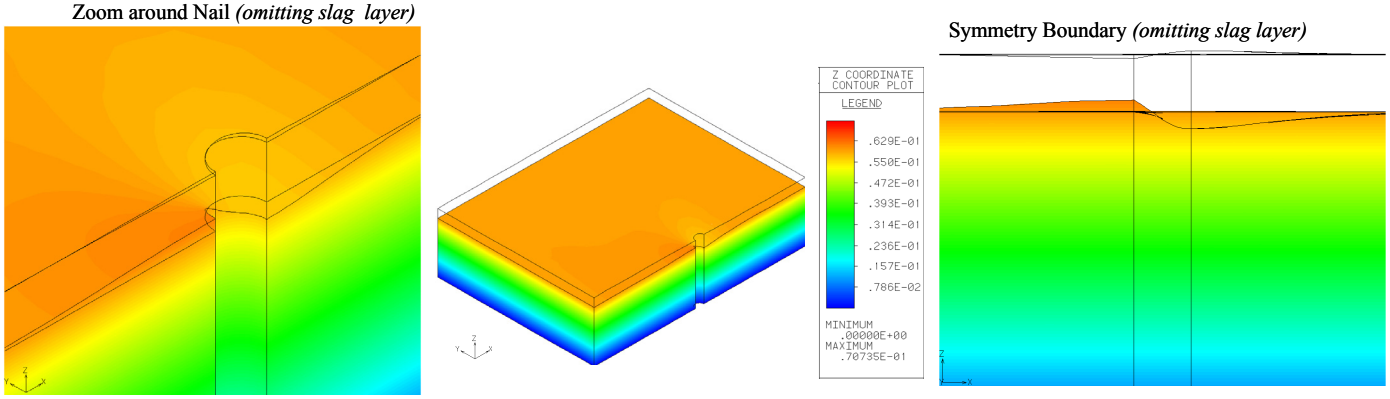

b) With slag (but slag layer not shown)

Figure 9. Surface deformation profile and vertical (z) velocity contours: 3 views (0.3 m/s; 10-mm diameter nail)

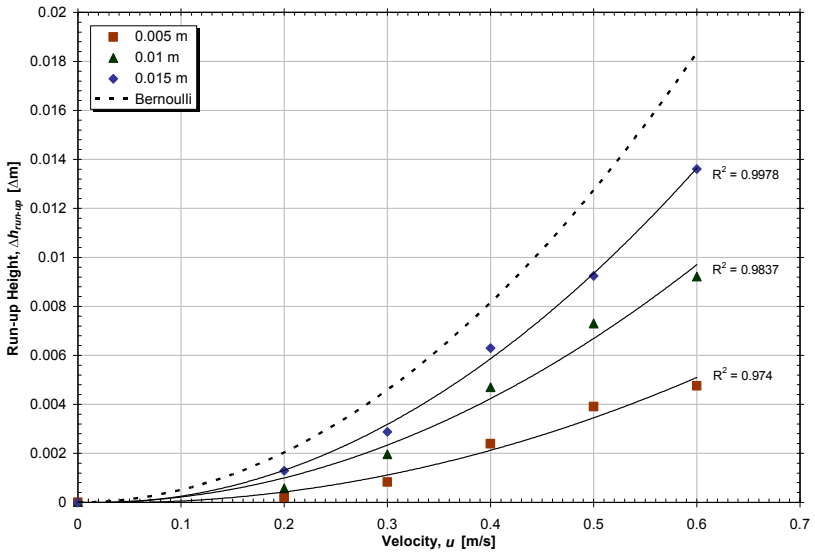

Figure 10. Leading edge run-up (with slag)

Effect of Fluid Properties

Several simulations were performed to compare the runup heights and profile shapes produced for different fluids and conditions. Table I shows the properties of steel and slag used in the comparisons. Although its kinematic viscosity is similar to steel, water has a 7X lower density and 22X lower surface tension. The shapes of the free surfaces for both water and steel (without slag) in Fig. 11 look nearly identical in regions of low surface curvature far from the nail. Near the nail (which is designated by the two vertical lines in the figure) where the curvature is high, however, the steel model has a much less distorted free surface profile than the water. Again, this is due to the high surface tension of the molten steel; the changes in fluid elevation and sharp surface gradients are more restricted with a higher surface tension. For this reason, a physical water model cannot be used to model free surface behavior in molten steel.

Effect of Slag Layer

The effect of adding a slag layer (Slag Model) is also shown in Fig. 11, relative to a free-flowing steel surface (No-Slag Steel). Because displacing slag takes less potential energy than lifting the steel surface in air, height changes are easier. At the same time, the high viscosity of the slag layer greatly slows down the interface velocity. The latter effect predominates for small diameter nails, where flow is mainly directed around the nail, so the net result is decreased height changes. For larger nails, the former effect is stronger, so there is little difference in the liquid steel surface height and shape whether a slag layer is present or not.

Evaluation of Pressure Approximation

Several previous studies have found that height changes along a free surface can be estimated from the pressure distribution using energy conservation: $\Delta Height = p - p_o \big/ g\left(\rho_{steel} - \rho_{slag}\right)$ [26-28]. The shapes around the nail predicted with these "pressure approximations" are included in Fig. 11. Although the shape is correct, the approximations greatly overpredict the level variations, owing to their neglect of the curvature-restricting effect of surface tension over these short distances.

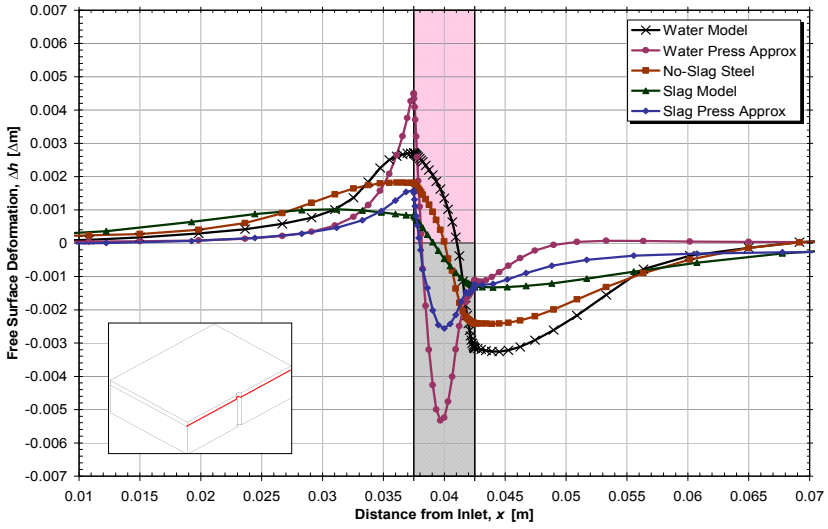

Figure 11. Comparison of interface surface shapes predicted in water and steel (No-Slag, 5-mm diameter, 0.3 m/s)

Solidified Knob Shape

The shape of the solidified knob can reveal a great deal about the local flow conditions when it formed. The shapes for the complete parametric study (varying surface velocity, nail diameter, and slag presence) are provided in Fig. 12. The shape depends on a force balance between boundary layer flow velocity, gravitational forces, surface tension, and leading edge run-up. Without slag, the interface profile has a distinctive curved shape, which varies significantly with changing velocity. With slag, the profiles are almost linear, with a slope, $^{dz}/_{dx}$ = -0.78, so cannot be used alone to indicate velocity.

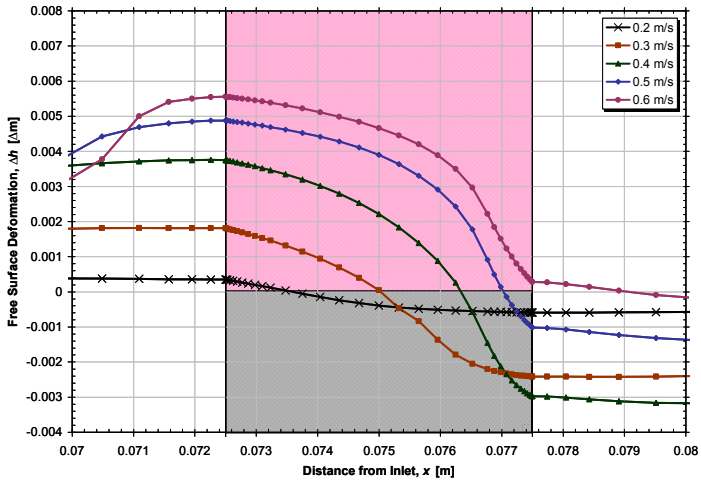

a) No Slag; 5-mm nail

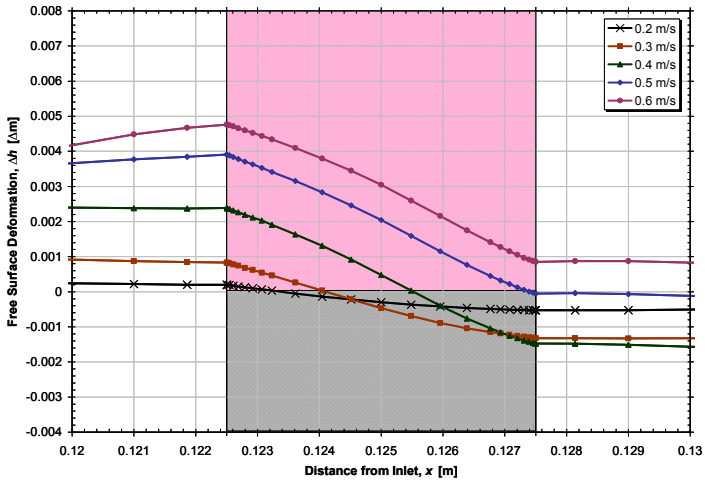

b) With Slag; 5-mm nail

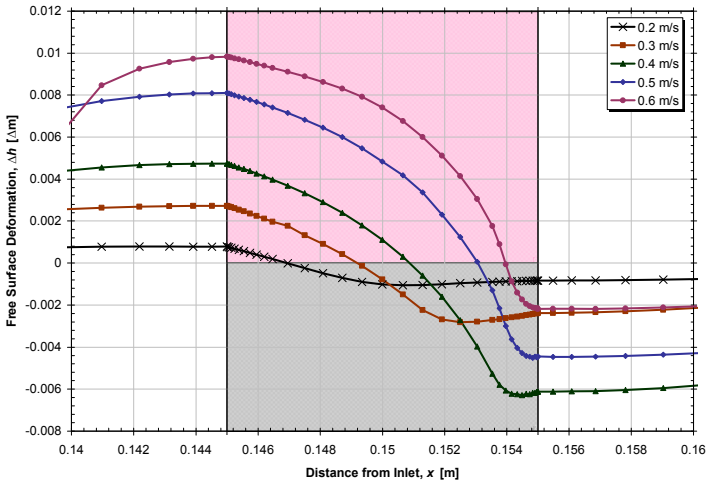

c) No Slag; 10-mm nail

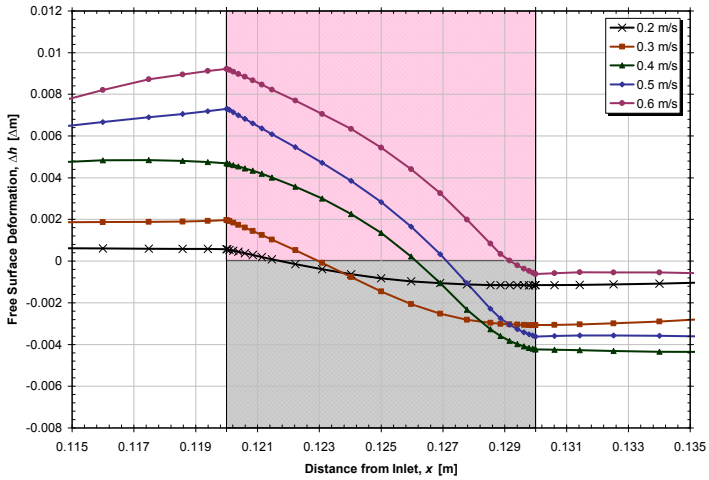

d) With Slag; 10-mm nail

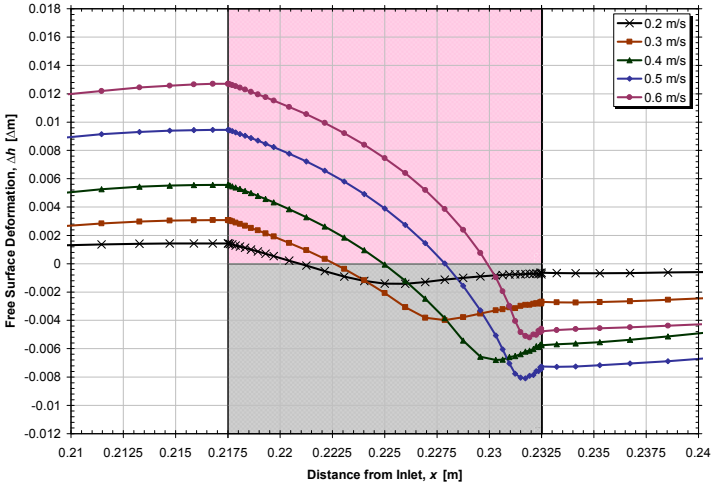

e) No Slag; 15-mm nail

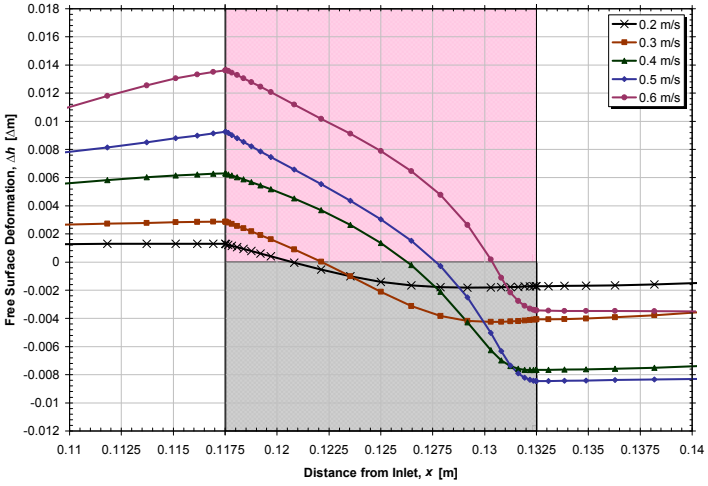

f) With Slag; 15-mm nail

Figure 12. Solidified knob profile shapes predicted in flowing steel with and without a slag layer for nails with different diameters.

As the nail diameter increases, the flow cannot sustain an elevated free surface level all around its perimeter to the end of the knob. In these situations, the wake region forms prior to the knob end. At high velocities, this causes the free-surface level to rise before the flow is completely past the nail. A "lip" is formed at the downstream side of the knob, as evident in the 15-mm nail at every speed (Figure 12e). This lip has been observed on a few large-diameter nail samples taken from actual casters.

The runup height always increases consistently with increasing velocity (see Fig. 12). Unfortunately, it is difficult to measure. It should be possible to estimate for steel velocity knowing the entire knob profile shape and diameter, but it is difficult to compare the entire profiles quantitatively. An alternative, simpler method to estimate flow velocity is to simply measure the height difference between the maximum runup height at the front of the nail, and the minimum height at the back. Because the curvature of the profile also increases with velocity, however, the knob height reaches a maximum, which is found in Fig. 13.

The surface velocity can be quantified from the measured knob height, as given in Fig. 13. At slow velocities ($\leq$ 0.2 m/s), the runup height is small, so the profile is very flat and the knob height difference is too small to measure. In the developing region, the height difference increases almost linearly with casting speed, which spans the top surface velocity range of important practical interest. Large diameter nails produce the least ambiguous results.

With very high velocities, (> 0.6m/s), the effect of gravity is smaller than the boundary layer momentum, so the height of the wake region increases. This decreases the height difference, once the velocity exceeds a critical value, and is defined as the "overdeveloped" region in Fig. 13. The critical velocity is smaller for nails with smaller diameters. This is because the shorter travel distance around the nail allows the boundary layer flow to retain its momentum, and dominate over gravity at smaller velocities. Further increase in surface velocity actually causes the knob height difference to decrease: gravitational force becomes negligible compared to boundary layer momentum, so the flow maintains a more horizontal trajectory past the nail.

Quantifying Surface Velocity

Fig. 13 can be used as a chart to find the local surface velocity at each nail of a nailboard test. The runup height difference is first measured between the maximum and minimum heights on opposite sides of the knob. These heights are best measured where the knob intersects with the nail surface, which is where the first liquid solidified. Measuring the maximum height of the knob (usually further away from the nail) is also possible, but the effective diameter becomes the diameter of the lump where the heights are measured. In either case, the surface velocity is read directly from Fig. 13b) for powder casting, interpolating between the lines as necessary to find the appropriate column diameter. Fig. 13a) can be used for casting with oil lubrication (without slag).

Small knob height differences (< ~2mm) indicate slow surface velocities (<0.2m/s). Very large knob height differences indicate high-speed flow. Intermediate knob-height differences give a quantitative measure of surface velocity in the developing range between ~0.2-0.5m/s: ~the same range that is optimal for casting quality. Adjustments must be made to the knob height difference if the nail is not quite vertical to the liquid level. This can happen if there is a large variation in surface profile, or if there are local surface waves.

CONCLUSIONS

This paper presents a relation to quantify liquid velocity along the top surface of a molten metal bath using nail board measurements. The results are based on a mathematical model of flow past a submerged nail that incorporates 3-D, turbulent, multi-liquid flow and the shape of two independent free-surfaces, including the effects of surface tension and gravity. Relations between knob profiles and surface velocity are found as a function of nail diameter, both with and without the presence of a top-surface viscous slag-layer cover. The model was verified with test problems including water-model measurements and applied to simulate knob profiles in a molten steel environment. The following are specific findings:

1. The leading edge run-up on the knob increases in proportion to the square of the inlet velocity. Increasing knob diameters yield leading edge run-ups close to the upper energy-balance limit of the Bernoulli relation. If it can be measured, the leading edge height provides a clear indication of metal velocity, both with and without the slag layer, especially for high velocity (> 0.3 m/s), and large nail diameter (> 10 mm).

2. The knob height difference (measured as the leading edge run-up height minus the trailing edge run-down height at the nail surface) provides a unique indication of velocity near the surface of the molten metal. This height difference increases almost linearly within the velocity range from 0.2 to 0.5 m/s. Within this region, knob height differences can be used to accurately determine free-stream velocity in the steel plant, knowing the nail diameter.

3. Without a slag layer, the shape and curvature along the knob free surface are distinctly different for each velocity/diameter case, thus providing another unique indicator to confirm fluid velocity.

4. With a slag layer, the steel/slag interface profile is constrained to be almost linear. Because the knob profile is nearly identical for each case, the shape alone cannot be used to indicate velocity.

5. Water models do not approximate steel Nailboard tests: the free surface profiles are much steeper and height differences larger than those in steel, due to the smaller surface tension.

6. Pressure/height approximations greatly overestimate the free surface deformation (by up to an order magnitude), owing to the neglect of surface tension effects.

7. Optimum nail submersion time decreases with smaller nail diameter. Excessive immersion times produce remelting of the lower knob, and detrimental mushrooming of the top due to surface solidification.

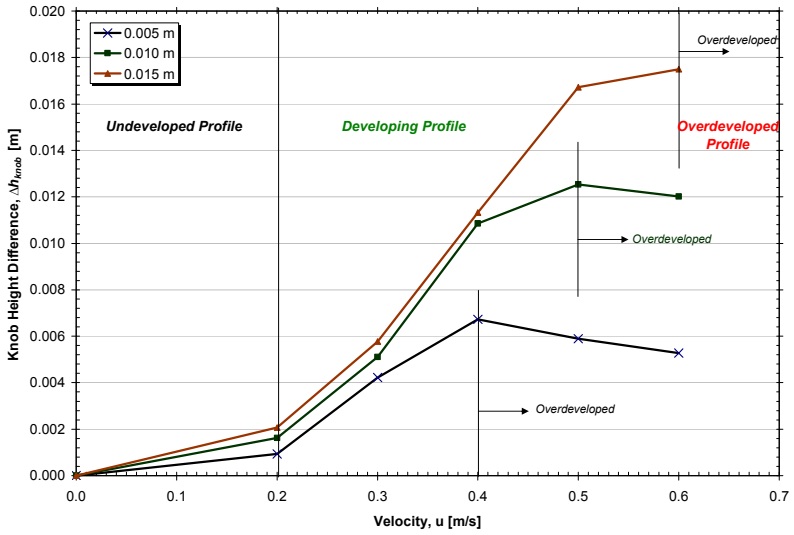

a) No Slag

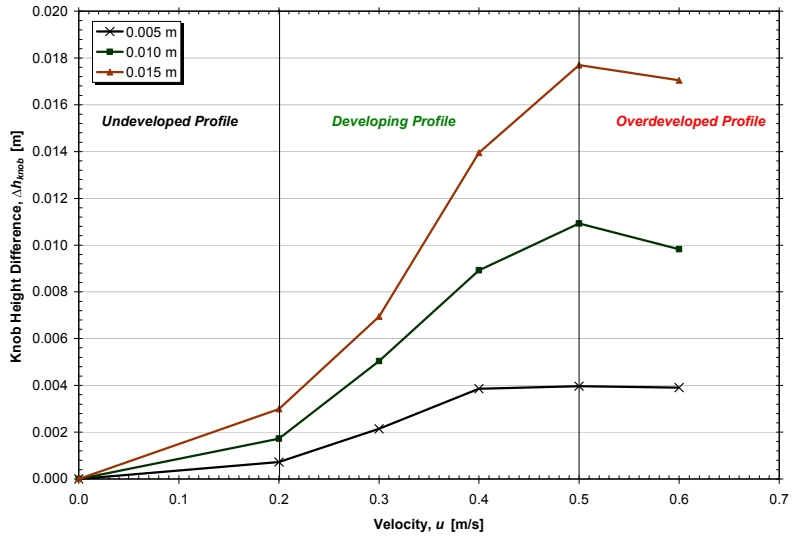

b) With Slag

Figure 13. Relation between steel surface velocity and measured height of knob from nail-board test

ACKNOWLEDGEMENTS

We wish to thank the member companies of the Continuous Casting Consortium at the University of Illinois for support of this research, and especially Ron O'Malley and Nucor, Decatur, Alabama for help in performing the plant measurements.

REFERENCES

1. P.H. Dauby, W.H. Emling, and R. Sobolewski, *Lubrication in the Mold: A Multiple Variable System.* Ironmaker and Steelmaker, 1986. **13**(Feb): p. 28-36.
2. Dauby, P.H., M.B. Assar, and G.D. Lawson, *PIV amd MFC Measurements in a Continuous Caster Mould. New Tools to Penetrate the Caster Black Box.* La Revue de Metallurgie - CIT, 2001. **98**(4): p. 353-366.
3. McDavid, R., *Fluid Flow and Heat Transfer Behavior of Top-Surface Flux Layers in Steel Continuous Casting*, in *Mechanical and Industrial Engineering*. 1994, University of Illinois at Urbana-Champaign: Urbana, IL.
4. McDavid, R. and B.G. Thomas, *Flow and Thermal Behavior of the Top-Surface Flux/ Powder Layers in Continuous Casting Molds.* Metall. Trans. B, 1996. **27B**(4): p. 672-685.
5. Thomas, B.G., *Chapter 14. Fluid Flow in the Mold*, in *Making, Shaping and Treating of Steel: Continuous Casting*, A. Cramb, Editor. 2003, AISE Steel Foundation, Pittsburgh, PA. p. 14.1-14.41.
6. Siebo Kunstreich, et al. *Multi-Mode EMS in thick slab casters molds and effect on coil quality and machine performance*. in *5th European Continuous Casting Conference, Nice, France, June 20-22, 2005*. 2005.
7. Cukierski, K. and B.G. Thomas, *Flow Control with Local Electromagnetic Braking in Continuous Casting of Steel Slabs.* Metals and Materials Transactions B, 2007(in press).
8. Y.K. Park and S.K. Baek, *Revamping of the No. 1-3 Slab Caster at POSCO Gwangyang: Design, Start-up and First Results.* La Revue de Métallurgie-CIT, 2004. **6**(June): p. 467-472.
9. Lee Sang-Min and K. Oh-Duck. *Electromagnetic stirring in the mold at the newly rebuilt Posco Pohang No. 3-3 machine* in *International Conference and Exhibition, ISS, April.* 2003. Indianapolis, IN.
10. Kubota, J., et al., *Meniscus Flow Control in the Mold by Travelling Magnetic Field for High Speed Slab Caster*, in *Mold Operation for Quality and Productivity*, A.W. Cramb and E. Szekeres, Editors. 1991, Iron and Steel Society: Warrendale, PA.
11. Emling, W.H., et al. *Subsurface Mold Slag Entrainment in Ultra Low Carbon Steels*. in *77th Steelmaking Conference Proceedings*. 1994: ISS, Warrendale, PA.
12. Jun Kubota, et al., *Steel Flow Control in Continuous Caster Mold by Traveling Magnetic Field*, *NKK Tech. Rev.*. 2001. p. 1-9.
13. Mikrovas, A.C. and A.C. Argyropoulos, *A Novel Technique to Estimate Velocity in Liquid Steel and in Other High Temperature Liquid Metals.* Trans. ISS, Iron and Steelmaker, 1993. **20**(10): p. 85-94.
14. Argyropoulos, S.A., *Measuring velocity in high-temperature liquid metals: a review.* Scand. J. Metall., 2000. **30**: p. 273-285.
15. Szekely, J., C.W. Chang, and W.E. Johnson, Met. Trans. B, 1977. **5B**: p. 514-517.
16. Szekely, J., *Experimental Study of Rate of Metal Mixing in Open-Hearth Furnace.* J. ISI, 1964. **202**: p. 505-508.
17. Melissari, B. and S.A. Argyropoulos, *Measurement of magnitude and direction of velocity in high-temperature liquid metals. Part II: Experimental measurements* Metall. Mater. Trans. B, 2005. **36**(5): p. 639-649.
18. Kohler, K.U., et al., *Steel Flow Velocity Measurement and Flow Pattern Monitoring in the Mould*, in *Steelmaking Conf. Proc.* 1995, ISS, Warrendale, PA: Nashville, TN. p. 445-449.
19. Thomas, B.G., et al., *Comparison of four methods to evaluate fluid velocities in a continuous slab casting mold.* ISIJ International (Japan), 2001. **41**(10): p. 1262-1271.
20. Iguchi, M., et al., *A New Probe for Directly Measuring Flow Velocity in a Continuous Casting Mold.* ISIJ Internat., 1996. **36**(Suppl.): p. S190-S193.
21. Rietow, B., *Investigations to Improve Product Cleanliness during the Casting of Steel Ingots*. 2007, University of Illinois at Urbana-Champaign: Urbana, IL.
22. Engleman, M.S., *FIDAP Theoretical Manual*. 2001, Fluent, Inc., 500 Davis Ave., Suite 400, Evanston, IL 60201.
23. G.X. Wu, R. Eatock Taylor, and D.M. Greaves, *The Effect of Viscosity on the Transient Free-Surface Waves in a Two-Dimensional Tank.* Journal of Engineering Mathematics, 2001. **40**: p. 77-90.
24. Forbes, L.K., *Critical Free-Surface Flow over a Semi-Circular Obstruction.* J. of Engineering Mathematics, 1988. **22**: p. 3-13.
25. Chaplin, J.R. and P. Teigen, *Steady Flow Past a Vertical Surface-Piercing Cylinder.* J. Fluids Structures, 2003. **18**: p. 271-285.
26. Panaras, G.A., A. Theodorakakos, and G. Bergeles, *Numerical Investigation of the Free Surface in a continuous Steel Casting Mold Model.* Metall. Mater. Trans. B, 1998. **29B**(5): p. 1117-1126.
27. Anagnostopoulos, J. and G. Bergeles, *Three-Dimensional Modeling of the Flow and the Interface Surface in a Continuous Casting Mold Model.* Metall. Mater. Trans. B, 1999. **30B**(6): p. 1095-1105.
28. Yuan, Q., B.G. Thomas, and S.P. Vanka, *Study of Transient Flow and Particle Transport during Continuous Casting of Steel Slabs, Part 1. Fluid Flow.* Metal. & Material Trans. B., 2004. **35B**(4): p. 685-702.